Mechanics & Industry **16**, 407 (2015)

DOI: 10.1051/meca/2015014
www.mechanics-industry.org

Mechanics & Industry

Study the effect of Gaussian and Uniform heat flux on laser forming of Bi-layer sheets

Mohammad Riahi[1], Mohamad Hoseinpour Gollo[2] and Seiied Nader Ameli Kalkhoran[1,a]

[1] Faculty of Mechanical Engineering, Iran University of Science and Technology, Tehran, Iran
[2] Manufacturing Engineering Department, Shahid Rajaee Teacher Training University, Tehran, Iran

Received 21 January 2014, Accepted 19 January 2015

Abstract – Laser forming process is one of the newest methods of sheet metal bending which no mechanical force needs. Although lots of investigations on laser forming process of mono layer sheet metals have been done, any experiments have not been conducted around bi- layer sheets. In this paper, laser forming process of bi-layer Al/SiC work pieces under Gaussian and Uniform heat distribution has been studied. Elastic-plastic temperature dependent material properties are considered. Also, the boundary condition is applied as free heat convection. The results of numerical simulations revealed that the amount of bending angle in Uniform heat flux distribution is always further than Gaussian distribution. In addition, temperature distribution diagram in Uniform heat flux is almost 5% further than Gaussian form, and the maximum temperature in the work piece is 6% larger. For validation of numerical analyses, experimental tests are done by an Nd: YAG laser on bi-layer Fe/Al sheets. The amounts of bending angles are so close to the results of simulation. The average of the bending angle is almost derived 0.0038 Degree/ Watt in these experimental tests.

Key words: Laser forming / Cermet / Gaussian distribution / Uniform distribution

1 Introduction

Laser forming is a new phenomenon which is created by thermal stress by Laser radiation throughout a sheet [1]. A set of Laser parameters such as: power, wave length, diameters, velocity of Laser radiation, absorption coefficient, specific heat, conductivity and expansion coefficient affect the forming procedure [2, 3]. For the first time, Vollertsen [2] and Geiger [3] have discovered and suggested three different mechanisms to express thermo-mechanical behavior of materials, which were Temperature Gradient Mechanism (TGM), Buckling Mechanism (BM) and Upsetting Mechanism (UM). This method could be widely used in rapid prototyping, automotive manufacturing, aerospace and ship building [2, 4–7]. Figure 1 shows the scheme of sheet bending due to laser radiation.

Although in most studies sheet bending has been considered along a straight line, however, some investigations have concentrated on the production of different geometrical shapes like spherical [8], Sattler shape [9, 10] and pipe bending [11–13]. So far, different materials have been examined numerically and experimentally by Laser forming process. Some of these materials are different types of steels [14–19], Aluminum [20–23], Titanium [24, 25], Copper [26, 27], Silicon [28] and Chromium [29]. In association with forming of cermet sheet (Al/Sic) by Laser forming process, Shen et al. [30] performed a numerical study in 2009. This bi-layer cermet sheet combined the characteristics of Aluminum and Ceramic and while having anti-erosion and strength capability of Ceramic, it also contains all natural properties of Aluminum. Principle disadvantage of this material is in its weak formability which causes a limitation in its utilization for a vast number of applications. Regarding simulation of heat flux of Laser radiation, different models have been recommended, the most recognized of which are Gaussian and Uniform heat distribution.

In this paper, numerical investigation of LF process under two distributions of Gaussian and Uniform on bi-layer sheets of Cermet comprised of Aluminum 6061 and SiC Ceramic is investigated. Temperature distribution and plastic strain on the surface and thickness of the workpiece were the parameters that were scrutinized and studied herein. Results indicated that heat distribution was very close and almost equal on both Aluminum

[a] Corresponding author: naderameli@gmail.com

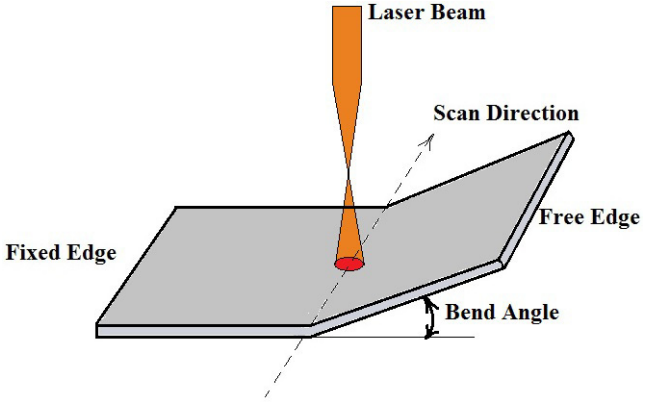

Fig. 1. Schematic of metal forming procedure by using Laser radiation.

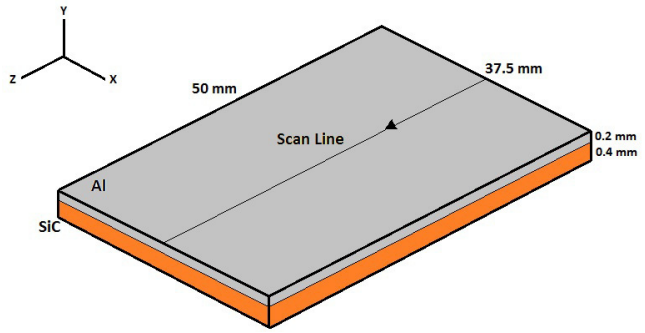

Fig. 2. Schematic of cermet piece.

surfaces. However, due to low thermal diffusivity of ceramic, when the heat flux was applied on the ceramic surface, the amount of temperature at the lower surface of ceramic layer was less than other surfaces and a short time after passage of laser radiation, reaches its maximum. In the end, in order to evaluate the simulation procedure, a set of experiments was done by a 300-watt Nd: YAG laser

2 Finite element simulation

2.1 Geometry modeling

The studied workpiece in this investigation was a bi-layer cermet made from Al/Sic. Its dimension is 37.5 × 50 mm and the thickness of metallic and ceramic layer was 0.2 mm and 0.4 mm. Figure 2 shows geometrical dimensions of the part. In this study, it was assumed that primarily workpiece was smooth and flat without any default.

2.2 Material properties

Another assumption which was made in the simulation was isotropic property of the workpiece. Since material properties are temperature-dependent, it is necessary to define different values in specific heat-span. The mechanical model of the Aluminum layer was assumed to be elasto-plastic and its data at different temperatures are shown in Tables 1 and 2.

Table 1. Yield stress and Young's modulus of Aluminum 6061 at different temperatures [31].

T (°C)	Yield stress (MPa)	Young's modulus (GPa)
20	125	70
100	95	70
200	55	61
300	27	55.6
400	15	49.3
500	5	41.3
600	5	5

Table 2. Specific heat, Density and Conductivity of Aluminum 6061 at different temperatures [31].

T (°C)	Specific heat (J/kg °C)	Density (kg.m^{-3})	Conductivity (W/m °C)
20	898	2750	170
120	951	2730	–
220	1003	2710	–
320	1055	2690	–
420	1108	2660	–
587	1195	2630	221
644	1200	2450	–

Table 3. Mechanical and thermal properties of Ceramic at room temperature 20 °C [32,33].

Properties	SiC
Specific heat (J/kg °C)	630
Thermal conductivity (W/m °C)	0.32
Coefficient of thermal expansion (10^{-6}/°C)	3.8
Young's modulus (GPa)	450
Poisson's ratio	0.17
Density (kg.m^{-3})	3230

According to the obtained results, the generated stress in the ceramic layer was always less than its yield stress. Therefore, this layer always remains in the elastic region. Consequently, the ceramic layer model was assumed to be perfect elastic. Properties of ceramic are given in Table 3.

2.3 Heat flux distribution

In light of the fact that origin of all occurring in a Laser Forming process is heat distribution, thus, review of all models of heat fluxes would be of high importance. A real heat distribution of laser radiation is shown in Figure 3. As can be seen, the real heat flux distribution is between Gaussian and Uniform model. Accordingly, some researchers use the Gaussian model and others use Uniform model in their researches. This profile shows that concentration of heat flux is in the center of radiation and, by moving away from it, the heat flux is exponentially decreased.

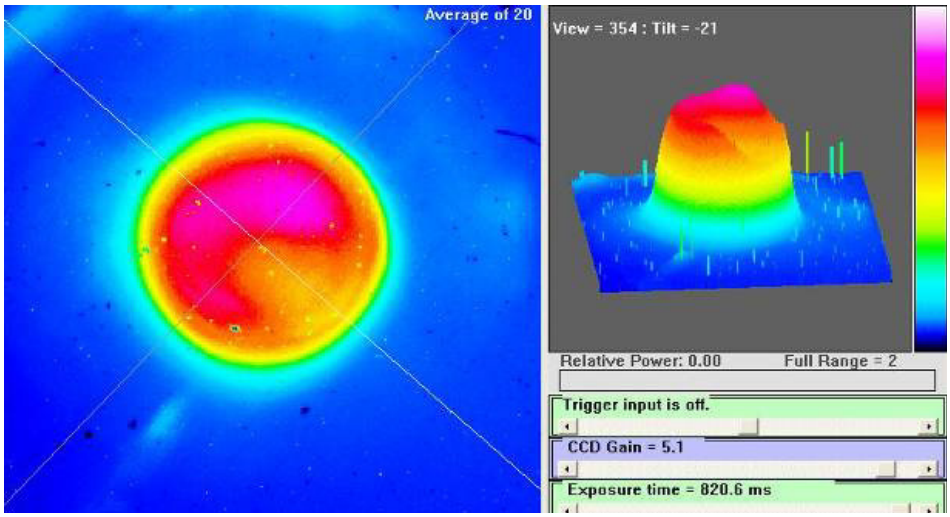

Fig. 3. Laser radiation profile in form of Gaussian distribution with 150 watt power.

Mathematical equation of Gaussian heat flux distribution is as follows [22]:

$$I(x,y) = \frac{2P}{\pi r_0^2} exp\left(\frac{-2\left[(x-x_0)^2+(y-y_0)^2\right]}{r_0^2}\right) \quad (1)$$

In which P is the laser's power, r_o is the radius of laser beam and (x_0, y_0) is coordinate of the laser beam center.

Uniform heat flux distribution is another model which has been used by some researchers to simulate the used heat flux of laser [34,35]. In this model, laser beam heat flux is applied to a surface with uniform intensity. Equation of this type of heat flux distribution is:

$$I(x,y) = \frac{P}{\pi r_0^2} \quad 0 \le r \le r_0 \quad (2)$$

In conducted numerical simulation, both types of heat fluxes were studied and their results were compared. Indeed, a very important point was to maintain the part's temperature below its melting temperature. In this process, no external mechanical force was exerted on the part and also this part was assumed to contain no residual stress what so ever.

2.4 Boundary conditions

In this process, one of the edges parallel to the scanning path of laser along Z direction was fixed. As the amount of radiation was negligible in this analysis, boundary condition all over the surfaces of the part was only assumed free convection, in which convection heat transfer coefficient was 12 W/(°C.m^2) and ambient temperature was 25 °C. The amount of heat transfer from sheet's surfaces was according to the following equation:

$$q_c = h_c(T_s - T_0) \quad (3)$$

In this equation, h_c is the heat transfer convection coefficient; T_s is part's initial temperature and T_0 is the ambient temperature.

2.5 Mesh selection of part

In laser forming process, the region under the laser beam and small vicinity of it, is the only area which has experienced the plastic strain; and the other regions do not have significant effect on the final result of process. As a result, fine mesh was applied under the laser beam area. In order to increase the precision of the solution, meshing of the area affected by heat flux was selected as hexahedral in the following, to reduce the analysis time of the software; further elements were selected as tetrahedral and larger in dimensions. In all conducted simulations, 3-D linear element and eight nodes (C38DT) were used. By changing the number of nodes and the type of meshing, the analysis of mesh sensitivity has been carried out and its result is shown in Figure 4a. Overall, final elements number of the workpiece was equal to 19 328. Figure 4b shows the meshing of the workpiece.

2.6 Solution condition

Solving this problem was in the form of coupled thermal-mechanical model. In order to increase the precision of analysis, nonlinear solution was used. Cooling time of the sheet after passing the laser radiation was assumed as 5 s. Because of the subroutine coding in the analysis of laser forming process, only one step has been defined in the software. Value of power, scanning speed, beam diameter and path of scanning depending on the designated simulation were applied in the code writing section of the software.

In Abaqus/Standard the temperatures are integrated using a backward-difference scheme, and the nonlinear coupled system is solved using Newton's method. This software offers an exact as well as an approximate implementation of Newton's method for fully coupled temperature-displacement analysis.

An exact implementation of Newton's method involves a nonsymmetric Jacobian matrix as is illustrated in the

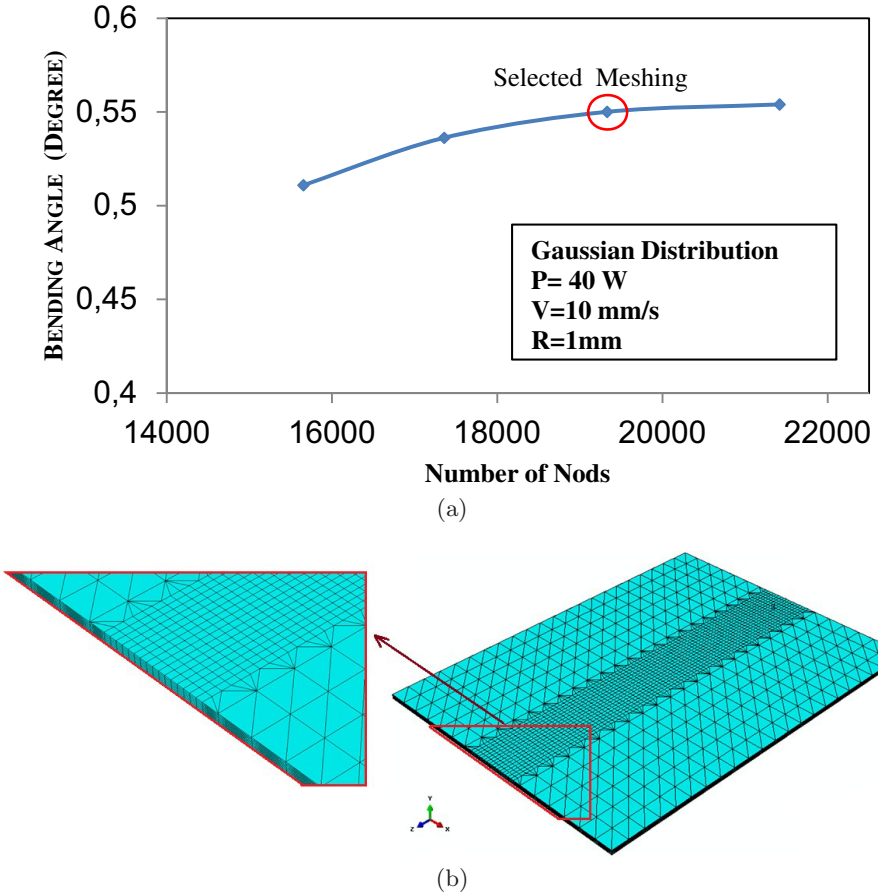

Fig. 4. (a) The trend of mesh sensitivity. (b) Workpiece Meshing.

following matrix representation of the coupled equations:

$$\begin{bmatrix} K_{uu} & K_{u\theta} \\ K_{\theta} & K_{\theta\theta} \end{bmatrix} \begin{Bmatrix} \Delta u \\ \Delta\theta \end{Bmatrix} = \begin{Bmatrix} R_u \\ R_\theta \end{Bmatrix} \quad (4)$$

where Δu and $\Delta\theta$ are the respective corrections to the incremental displacement and temperature, K_{ij} are submatrices of the fully coupled Jacobian matrix, and R_u and R_θ are the mechanical and thermal residual vectors, respectively.

Solving this system of equations requires the use of the unsymmetric matrix storage and solution scheme. Furthermore, the mechanical and thermal equations must be solved simultaneously. The method provides quadratic convergence when the solution estimate is within the radius of convergence of the algorithm. The exact implementation is used by default [36].

3 Discussion

It could be definitely stated that the main parameter in LF process is heat transfer and heat distribution. Therefore, studying of these parameters is of utmost importance. In Figure 5, temperature gradient of the workpiece along its thickness and at its center under Gaussian heat flux is shown.

It is evident that maximum temperature was at the surface of the workpiece at the center of laser radiation. Also in this place, temperature gradient at the upper layer, which was made of Aluminum, was negligible. Probably, this issue was stemmed from the fact that this layer's thickness was so thin and the concentration of heat flux was minute. Passing of this layer, due to ceramic's low conductivity and temperature at the lower surface, dropped intensely.

In Figure 6, heat distributing along the same direction is shown for Uniform heat flux. It is noticeable that maximum temperature of both conditions was almost equal. However, area of maximum temperature surface in Uniform heat flux was larger than for Gaussian heat flux, which could be in concentration of heat flux of Gaussian distribution in an area smaller than the diameter laser radiation.

Temperature distribution on the surface of the workpiece and at different stages of the process for two assumed types of heat flux is shown in Figure 7. Heat distribution on the workpiece's surface for both heat fluxes was almost equal. However, area of surface with maximum temperature was larger in the Uniform heat flux.

The main difference between Gaussian heat flux and Uniform one was in the produced bending angle in the workpiece. Figure 8 shows displacement contours at

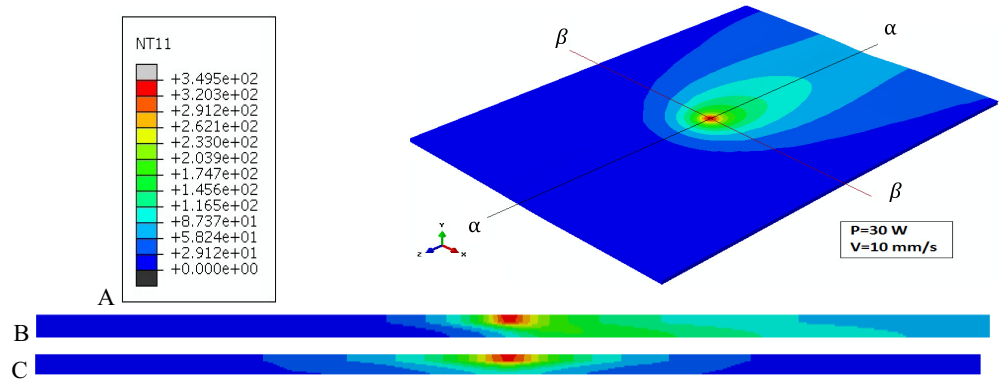

Fig. 5. (A) Temperature distribution by Gaussian heat flux, (B) Along $\alpha - \alpha$ and (C) Along $\beta - \beta$.

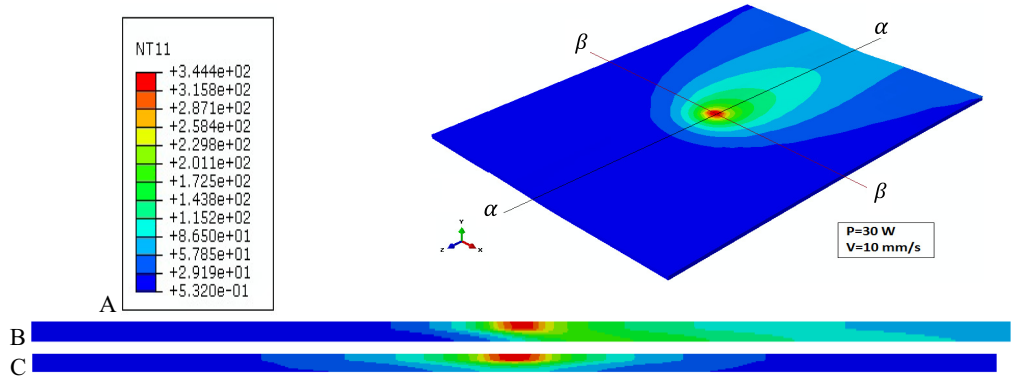

Fig. 6. (A) Temperature distribution by Uniform heat flux, (B) Along $\alpha - \alpha$ and (C) Along $\beta - \beta$.

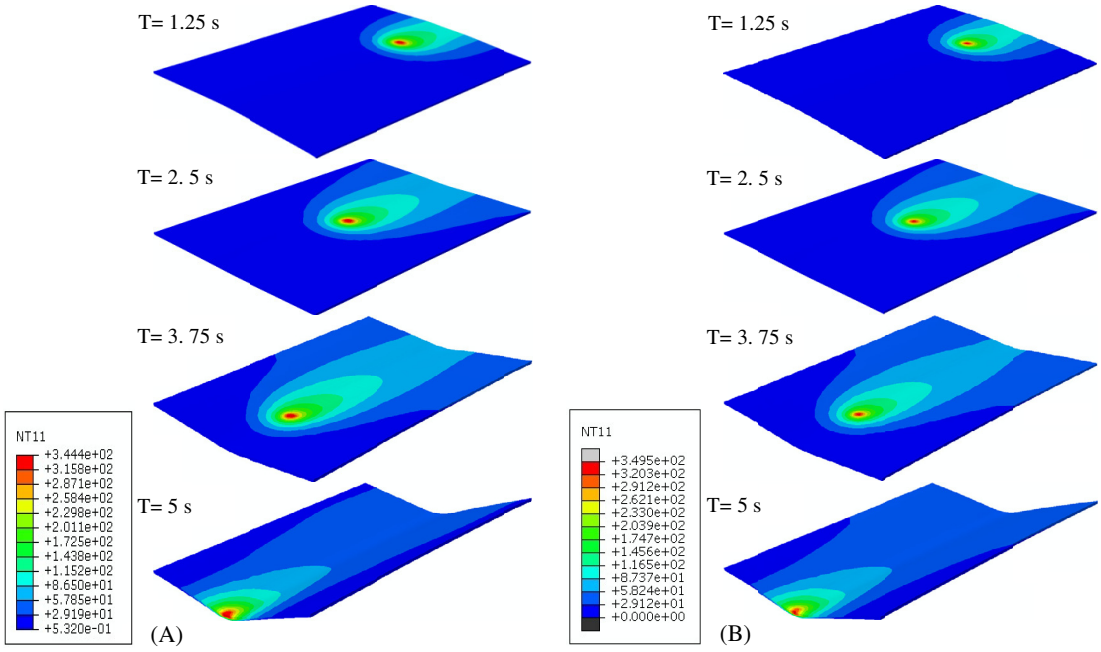

Fig. 7. Heat distribution on the surface of the workpiece in different stages (A) for Uniform heat flux and (B) for Gaussian heat flux ($P = 30$ w, $V = 10$ mm.s^{-1}).

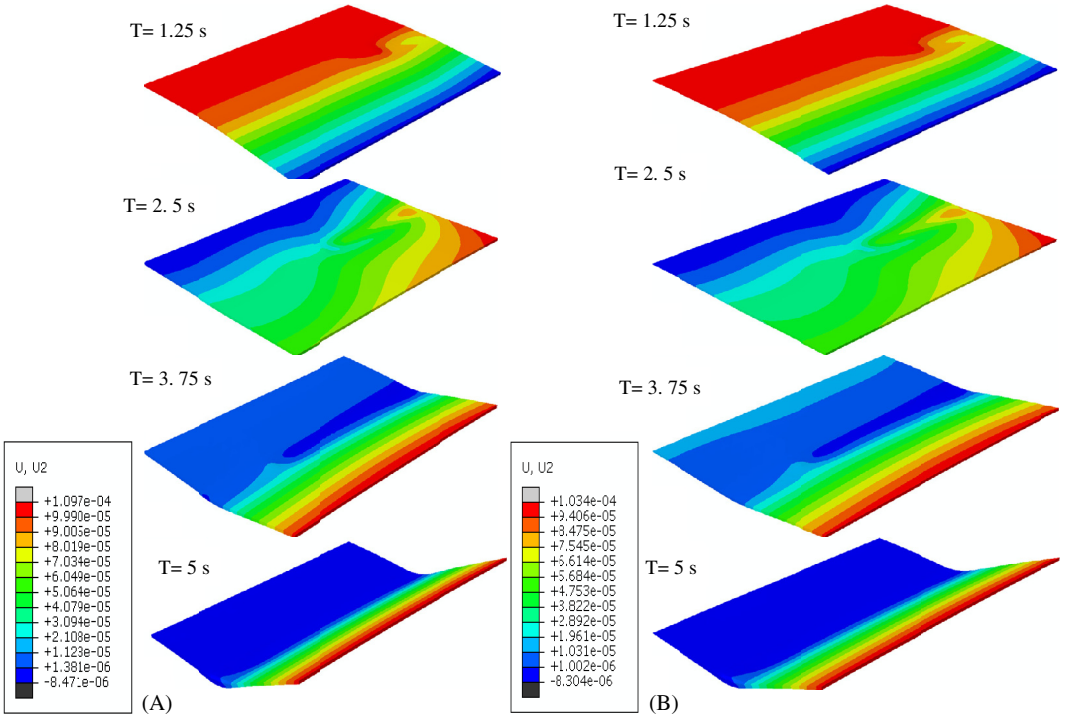

Fig. 8. Plastic deformation of workpiece in different stages. (A) for Uniform heat flux and (B) Gaussian heat flux ($P = 30$ W, $V = 10$ mm.s^{-1}) .

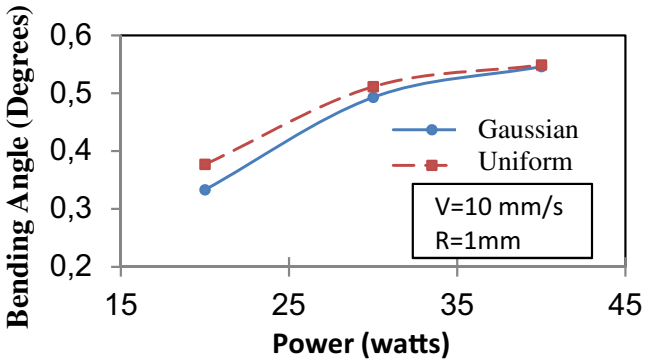

Fig. 9. Changes in bending angle for Gaussian and Uniform distribution of laser heat flux in different laser powers.

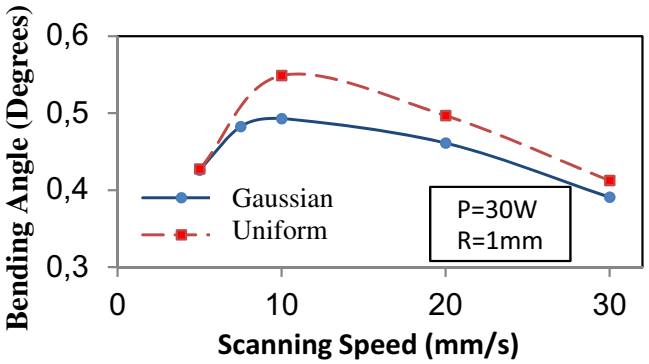

Fig. 10. Changes in bending angle for Gaussian and Uniform distribution of laser heat flux in different scanning speeds of laser.

different time durations of laser beam pass, in which Figures 8A and 8B are respectively related to Uniform and Gaussian heat flux distribution. Initially, by starting the laser beam movement, a small counter bending is seen and in the following, positive bending started to grow up to the end of process.

Obtained results under different conditions including change in power, scanning speed and laser beam diameter are indicative the point that sheet plastic deformation under Uniform heat flux was always more than its value in the laser with Gaussian heat flux distribution.

Figures 9–10 depict changes in the bending angle of the sheet in laser forming process at different powers and scan speeds. Figure 9 shows that, with increasing in the laser's power, sheet's bending angle also increased, which could be because by increasing the laser power, more heat gradient along sheet's thickness has been caused and eventually leads to increase in the bending angle. Figure 10 represents the presence of optimized point for bending angle at different speeds of laser scanning. The reason for decrease in bending angle at speeds higher than optimized one was related to the decrease in heat gradient along thickness. By reducing the scanning speed, it could be safely stated that the whole sheet thickness was equally heated in the scanning location. As a result, for heat gradient subsequently, its bending angle decreased.

Figure 11 shows the changes in bending angle caused by different laser beam diameters. In Figure 11A, by keeping the speed and power of laser fixed, laser beam

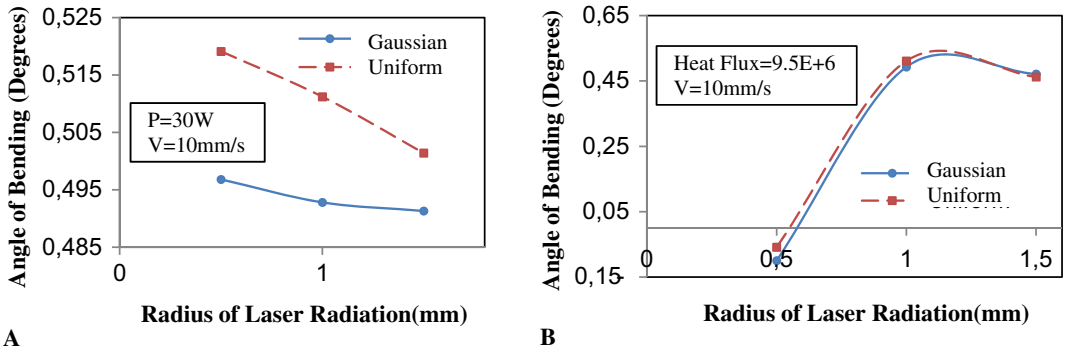

Fig. 11. Changing in bending angle for Gaussian and Uniform distribution in different laser beam diameters. (A) In constant power condition. (B) In constant heat flux.

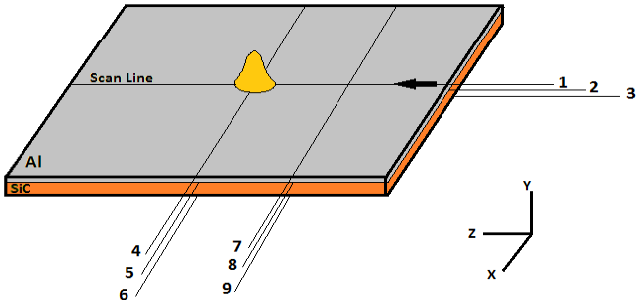

Fig. 12. Studied paths of temperature distribution.

diameter changed and bending angles were obtained under two types of Gaussian and Uniform heat flux. It is evident that increasing beam diameter in both types of heat distribution caused reduction in the bending angle, because despite enlargement in beam diameter, the same constant power was applied to a larger area and hence, reduction in heat gradient and subsequently decrease in the final bending angle were deduced. In Gaussian heat distribution, maximum generated heat was concentrated in the center of radiation. For this reason, in comparison with Uniform heat distribution, a smaller area would be involved in the procedure of plastic deformation and thus the produced bending angle would be smaller.

Figure 11B shows a different result from the previous case. In this condition, since heat flux was constant, by increasing laser beam, more heat power would be applied to the surface. As a result, consequenty, heat strain increased and eventually, larger bending angle is obtained. Also, if heat power surpassed its optimized point, heat distribution along sheet thickness would become smoother and heat gradient decrease. Consequently, final bending angle also decreased.

In order to study temperature distribution at different points of the workpiece, the defined paths in Figure 12 were selected. Values related to Gaussian and Uniform heat flux distribution just when laser beam scanned exactly half of the path, have been shown in Figure 12.

As far as the three paths of 1, 2, and 3 were concerned, as was expected, maximum temperature was along path 1. However, due to low thickness of Aluminum layer, it is evident that heat gradient in this layer was negligible and temperature of upper and lower surfaces of this layer was the same almost along all path length (paths 1 and 2). On the other hand, since lower ceramic layer had less conductivity, heat along thickness of this layer transferred slower and, for this reason, the lower surface (path 3) reached its maximum temperature a short time after passing of laser radiation from its upper surface.

Paths 4 to 9 are symmetric with respect to "Plane ZY". Hence the diagrams are also symmetric in these paths. Comparing two types of heat flux in these paths made it evident that theses heat diagrams under Uniform heat flux were almost 5% wider than those obtained from Gaussian heat flux and their maximum temperature was on average 6% larger. Reason for this is the larger area of maximum heat flux in Uniform heat distribution. Similar to analysis provided in the case of path 3, as expected, temperature of path 6 was less than of the two upper surfaces and temperature of path 9 was more than its two upper surfaces.

4 Validation

Due to the limitation in the availability of the Cermet sheet, experimental tests were done for bi-layer Fe/Al with the total thickness of 2.105 mm and dimensions of 60×105 mm^2. The thickness of each layer was measured by an optic microscope that is shown in Figure 14. Thickness of Fe layer was 1.455 mm and that of Al layer was 0.650 mm.

In order to form this sheet, an Nd: YAG laser, model HAN*S LASER with the maximum power of 300 W was used. The available ranges for the laser parameters are 1–1000 Hz for pulse frequency, 0.02–20 ms for pulse duration, and 0–30 J for pulse energy. The experiments were conducted with frequency of 29 Hz and workpiece velocity 7 mm.s^{-1}. Two major factors were important for selecting 29 Hz frequency: the first factor was the required overlapping of alternative laser pulses, regarding process travel speed and absolute irradiated energy per unit length of the workpiece. The second factor was limitations of laser source that confined the present choices

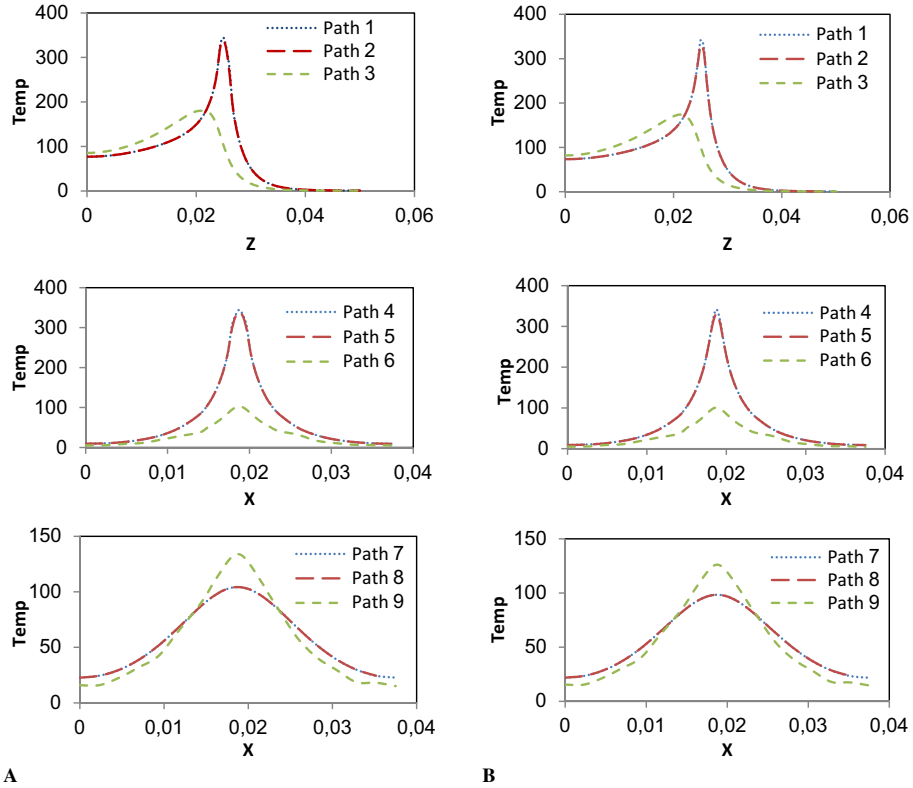

Fig. 13. Temperature distribution of the workpiece along different paths: (A) For Uniform heat flux, (B) for Gaussian heat flux.

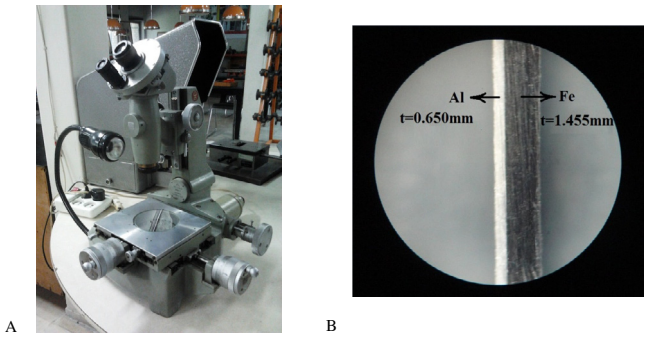

Fig. 14. (A) The optic microscope that is used for measuring the thickness of the each layer, (B) An image of the sheet thickness.

Fig. 15. Experimental setup for 2D laser forming and formed specimens.

about each combination of laser pulse energy, pulse duration and frequency for each value of average output power. Experimental setup for 2D laser forming and formed specimens are shown in Figure 15.

Result of the simulations and experimental tests for a laser with 2.1 mm beam diameter and 11 ms pulse duration with scan velocity of 7 mm.s^{-1}, is shown in Figure 16. These results demonstrated good agreement among the numerical and experimental data.

5 Conclusions

In this paper, effects of two types of Gaussian and Uniform laser heat flux on different parameters are presented. Due to larger radiation area at maximum heat flux, Uniform heat flux always produces larger bending angle compared to that of Gaussian distribution. It was further revealed that by increasing laser power, bending angle will also increase. This increase is caused by higher temperature gradient in higher powers. Also, results indicated that reducing speed of laser up to a certain point, causes increase in the bending angle and thereafter, it

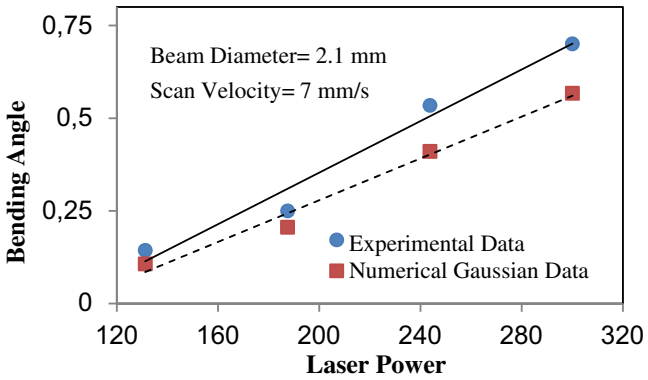

Fig. 16. Comparison between experimental and numerical results.

has reverse impact. Reason is that initially, by reduction in scanning speed, heat gradient in the sheet thickness increases, however, after certain time, reverse of this happens and bending angle decreases.

Variations in the laser beam diameter in two different conditions, by assuming constant laser power and thereafter by assuming constant heat flux in unit area were studied. In first condition, results indicated reduction in the bending angle by increase in the beam diameter and in the second condition, reverse of this happening. Of course, in condition of constant heat flux, by increasing in beam diameter, trend of increase stopped and a mild decrease began. This is for expansion in the surface temperature gradient and also due to the change in the nature of mechanism to BM.

Study of temperature distribution of sheet along thickness indicated that due to low thickness and high thermal diffusivity of Aluminum, temperature of the both upper and lower surface of this layer are almost equal. However, because of lower conductivity and specific heat in ceramic compared to Aluminum, lower surface of ceramic layer during heat flux application, would have lower temperature than its two upper surfaces. Also, due to lower rate of heat transfer in this layer, a little time after passing of laser beam from its upper surface, it will reach its maximum heat.

References

[1] Y. Namba, Laser forming in space, Proceedings of International Conference on Lasers, Las Vegas, 1985, pp. 403–407

[2] K. Scully, Laser line heating, J. Ship Prod. 3 (1987) 237–246

[3] Hong Shen, Frank Vollertsen, Modeling of laser forming – An review, Comput. Mater. Sci. 46 (2009) 834–840

[4] M. Geiger, H. Arnet, F. Vollertsen, Laser forming, Proceedings of the LANE (Laser Assisted Net Shape Engineering), 1994, pp. 81–92

[5] M. Geiger, F. Vollertsen, G. Deinzer, Flexible straightening of car body shells by laser forming International Congress and Exposition, Detroit, MI, USA, Published by SAE, Warrendale, PA, USA, 1993

[6] J. Magee, Laser bending of high strength alloys, J. Laser Appl. 10 (1998) 149–155

[7] G. Thomson, M.S. Pridham, Controlled laser forming for rapid prototyping, Rapid Prototyping Journal 3 (1997) 137–143

[8] T. Hennige, Laser forming of spatially curved parts, Proceedings of the LANE, 1997, pp. 409–420

[9] S.P. Edwardson, 3D laser forming of saddle shapes, Proceedings of the LANE, 2001, pp. 559–568

[10] J. Magee, K.G. Watkins, T. Hennige, Symmetrical laser forming, Proceedings of ICALEO, 1999, pp. 77–86

[11] N. Hao, L. Li, An analytical model for laser tube bending, Appl. Surf. Sci. 208 (2003) 432–436

[12] N. Hao, L. Li, Finite element analysis of laser tube bending process, Appl. Surf. Sci. 208-209 (2003) 437–441

[13] S. Safdar, L. Li, M.A. Sheikh, Z. Liu, Finite element simulation of laser tube bending: Effect of scanning schemes on bending angle, distortions and stress distribution, Opt. Laser Technol. 39 (2007) 1101–1110

[14] M. Hoseinpour Gollo, H. Moslemi Naeini, G.H. Liaghat, M.J. Torkamany, S. Jelvani, V. Panahizade, An experimental study of sheet metal bending by pulsed Nd: YAG laser with DOE method, Int. J. Mater. Forming 1 (2008) 137 –140

[15] M. Zohoor, E. Ghadiri Zahrani, Experimental and numerical analysis of bending angle variation and longitudinal distortion in laser forming process, Scientia Iranica B 19 (2012) 1074–1080

[16] L.J. Yang, J. Tang, M.L. Wang, Y. Wang, Y.B. Chen, Surface characteristic of stainless steel sheet after pulsed laser forming, Appl. Surf. Sci. 256 (2010) 7018–7026

[17] T. Ueda, E. SentokuYoshihiro Wakimura, A. Hosokawa, Flattening of sheet metal by laser forming, Opt. Lasers Eng. 47 (2009) 1097–1102

[18] M. Walczak, J. Ramos-Grez, D. Celentano, E.B.F. Lima, Sensitization of AISI 302 stainless steel during low-power laser forming, Opt. Lasers Eng. 48 (2010) 906–914

[19] B.S. Yilbas, A.F.M. Arif, B.J. Abdul Aleem, Laser bending of AISI 304 steel sheets: Thermal stress analysis, Opt. Laser Technol. 44 (2012) 303–309

[20] G.N. Labeas, Development of a local three-dimensional numerical simulation model for the laser forming process of aluminium components, J. Mater. Proc. Technol. 207 (2008) 248–257

[21] F. Quadrini, A. Guglielmotti, E.A. Squeo, V. Tagliaferri, Laser forming of open-cell aluminium foams, J. Mater. Proc. Technol. 210 (2010) 1517–1522

[22] I. Pitz, A. Otto, M. Schmidt, Simulation of the laser beam forming process with moving meshes for large aluminium plates, Phys. Proc. 5 (2010) 363–369

[23] M. Merklein, T. Hennige, M. Geiger, Laser forming of aluminium and aluminium alloys- micro structural investigation, J. Mater. Proc. Technol. 115 (2001) 159–165

[24] D.P. Shidid, M. Hoseinpour Gollo, M. Brandt, M. Mahdavian, Study of effect of process parameters on titanium sheet metal bending using Nd: YAG laser, Opt. Laser Technol. 47 (2013) 242–247

[25] Daniel F. Walczyk, Sameer Vittal, Bending of Titanium Sheet Using Laser Forming, J. Manufact. Proc. 2 (2000)

[26] D.V. Abramov, T.N. Gorudko, A.N. Koblov, D.S. Nogtev, O.A. Novikova, Laser Forming of Structures of Zinc Oxide on a Surface of Products from Copper Alloys, Phys. Proc. 5 (2010) 211–214

[27] Chao Zheng, Sheng Sun, Zhong Ji, Wei Wang, Jing Liu, Numerical simulation and experimentation of micro scale laser bulge forming, Int. J. Machine Tools Manufact. 50 (2010) 1048–1056

[28] Wang Xu-yue, Xu Wei-xing, Xu Wen-ji, Hu Ya-feng, LIang Yan-de, Wang Lian-ji, Simulation and prediction in laser bending of silicon sheet, Trans. Nonferrous Metals Soc. China 21 (2011) 188–193

[29] K.C. Chan, Y. Harada, J. Liang, F. Yoshida, Deformation Behaviour of Chromium Sheets in Mechanical and Laser Bending, J. Mater. Proc. Technol. 122 (2002) 272–277

[30] Hong Shen, Zhenqiang Yao, Jun Hu, Numerical analysis of metal/ceramic bilayer materials systems in laser forming, Comput. Mater. Sci. 45 (2009) 439–442

[31] Xian Luo, Yanqing Yang, Jiankang Li, Meini Yuan, Bin Huang, Yan Chen, An analysis of thermal residual stresses in SiC_f/Cu composites when TiC or Ni as binder, Mater. Design 29 (2008) 755–1761

[32] S.G. Long, Y.C. Zhou, Thermal fatigue of particle reinforced metal–matrix composite induced by laser heating and mechanical load, Compos. Sci. Technol. 65 (2005) 1391–1400

[33] J. Zimmerman, W. Wlosinski, Z.R. Lindemann, Thermomechanical and diffusion modeling in the process of ceramic–metal friction welding, J. Mater. Proc. Technol. 209 (2009) 1644–1653

[34] M. Hoseinpour Gollo, S.M. Mahdavian, H. Moslemi Naeini, Statistical analysis of parameter effects on bending angle in laser forming process by pulsed Nd: YAG laser, Opt. Laser Technol. 43 (2011) 475–482

[35] A.H. Roohi, M. Hoseinpour Gollo H. Moslemi Naeini, External force-assisted laser forming process for gaining high bending angles, J. Manufact. Processes 14 (2012) 269–276

[36] Abaqus 6.10 Documentation, Analysis User's Manual- Fully coupled thermal-stress analysis in Abaqus/Standard.